ELSEVIER

Solar Energy Materials and Solar Cells 32 (1994) 259–272

Solar Energy Materials and Solar Cells

Testing of dye sensitized TiO_2 solar cells I: Experimental photocurrent output and conversion efficiencies

Greg Smestad [a,*], Carlo Bignozzi [b], Roberto Argazzi [b]

[a] *Paul Scherrer Institute, Laboratory for Energy and Process Technology, CH-5232 Villigen-PSI, Switzerland*

[b] *Dipartimento di Chemica dell'Universita, Centro di Fotochimica C.N.R., 44100 Ferrara, Italy*

(Received 1 September 1993; in revised form 13 December 1993)

Abstract

Recently, a paper was published by the Lausanne Group headed by Dr. M. Graetzel which reported a simple low cost 7% efficient photo electrochemical solar cell made from a trinuclear Ru dye complex adsorbed on the very rough surface of a colloidal TiO_2 film. In the current paper, a verification of this result is presented using procedures described in the literature. Measurements are reported in simulated and natural sunlight which confirm that the efficiency is indeed in the range previously reported. Predicted Air Mass 1.5 photo currents are compared to those obtained from fabricated dye sensitized cells. Although current densities of 12 mA/cm^2 and voltages of over 0.6 V are measured, it is found that corresponding fill factors, less than 0.6, limit the performance of the cell under solar illumination. The basic economics of such a device are outlined and it is proposed that cell costs of $ 0.6 per peak watt could be possible if the longevity of the cell is at least 15 years.

1. Introduction

1.1. Background history and significance

In 1873, Herman Vogel [1] discovered that certain organic dyes could extend the green and red response of silver halide photographic films. The mechanism was later found to involve the electron or energy transfer from the organic chromophore to the semiconducting silver halide grain. This spectral sensitization, as it has come to be known, is the basis for modern photography. Photovoltaic cells have also been known for quite some time. The first was measured by E. Becquerel [2] in 1839 and employed copper oxide or silver halide coated metal electrodes

* Corresponding author.

SSDI 0927-0248(93)E0149-8

immersed in an electrolyte solution. Modern solar cells, on the other hand, are a more recent development, the first being developed in 1954 at RCA by Paul Rappaport and at Bell Labs by D. Chapin and G. Pearson [3]. These cells employed a solid state or p-n junction which marks the barrier between regions of electron and hole conduction. Electrons and holes created via the absorption of light in a silicon wafer diffuse at different rates in the n-doped and p-doped materials and are eventually collected at the junction. This p-n junction is formed by a process which resembles that used by the semiconductor industry to manufacture integrated circuits and computer chips. Potentially more cost effective technologies, which use thin films of such materials as amorphous silicon deposited on glass, are under development [4]. Although the equivalent of 50–60 MW of solar cells are currently produced each year [4,24,25], no technology has produced commercially available, efficient, reliable, and low cost modules that can be used on the exterior of buildings.

Using sensitization processes in solar cells has also been explored. Early work was done by researchers such as Meier, Tributsch, Memming and Gerischer [5]. Recently, a Swiss research group has combined several concepts to produce a low cost 7% efficient solar cell [6,7]. The cell, which is called a nanocrystalline dye sensitized solar cell, is remarkable in that it resembles natural photosynthesis in two respects: (1) it uses an organic dye to absorb light and transduce solar energy, and (2) it uses multiple layers to improve the absorption and collection efficiency over that of thicker layers. It is one of a new class of devices which are called molecular electronic devices [8]. To create the cell, a water solution of nanometer size particles of TiO_2 is deposited directly on conductive glass by a process similar to that used in painting. In fact, one of the cheapest known large bandgap semiconductors, this TiO_2 powder is primarily used in white paint. The film is heated to form a porous, high surface area TiO_2 structure which resembles a thin sponge or membrane. This is used as a support as the glass plate is dipped into a solution of a dye such as a red ruthenium carboxylated bipyridine complex or a green chlorophyl derivative [6,9,10]. A single layer of the dye molecules attaches to each particle of the TiO_2 via the carboxylic groups and acts as the primary

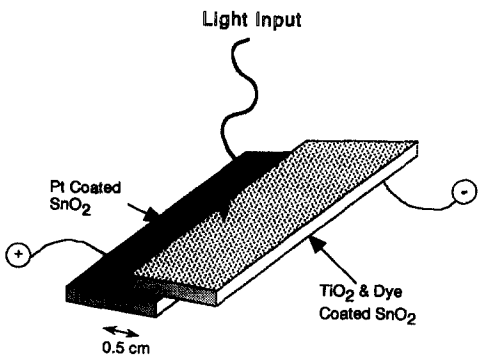

Fig. 1. Schematic of the dye cell construction showing the illumination through the dye coated TiO_2 layer. Note that the final solar cell active area is 0.5 cm^2.

Fig. 2. SEM of: (a) the rough colloidal TiO_2 surface at 100 K magnification. The TiO_2 particle size is between 10–50 nm, (b) the counter electrode surface at 60 K magnification showing the high surface area Platinum deposits on the larger SnO_2 grains.

absorber of sunlight. To form the final cell, a drop of liquid electrolyte containing iodide is placed on the film to percolate into the pores of the membrane. A counter electrode of conductive glass, which has been coated with a thin layer of platinum or carbon, is placed on top and the sandwich is illuminated through the TiO_2 support as shown in Fig. 1. Shown in Fig. 2a is an electron micrograph demonstrating the porous, high surface area, nature of the resulting TiO_2 films. Since the dye layer is so thin, the excited electrons produced from light absorption can be injected into the TiO_2 with near unity efficiency via sensitization. In contrast to conventional Si or GaAs solar cells, the mobility and charge carrier transport in the light absorbing compound is not relevant to the cell design. Previous use of thick layers of organic materials resulted in solar cells with low efficiencies since only a thin layer was involved in efficient charge collection [5]. What is new about the nanocrystalline cell is the use of a rough substrate for the dye in order to increase the light absorption while allowing for efficient charge collection. Because of the minute thickness of the dye, each layer of dye may not absorb very much light, but, like the leaves of a tree or the stacked thylakoid membrane found in photosynthesis, when added together, the many interconnected particles of the porous membrane can together absorb 90% of visible light [6,10]. The electrons lost by the dye are quickly replaced by the iodide in the electrolyte solution, to produce iodine or triiodide, which in turn obtains an electron at the counter electrode (see Fig. 3). The process is cyclic with the production of electrons which flow to the counter electrode through an external load to produce work. It has been reported that the final assembly has an overall sunlight to electrical energy conversion efficiency of 6–7% under direct sunlight

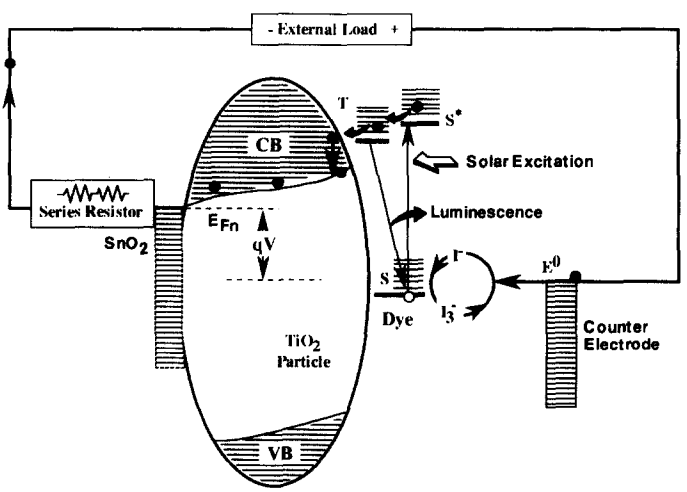

Fig. 3. Energy band diagram for an idealized TiO_2 dye solar cell. The electrons excited by light are rapidly injected into the conduction band, CB, of the TiO_2 where they are collected in order produce work in an external load. The excited dye is reduced by the iodide to produce iodine (or triiodide), which itself is reduced by the electron as it travels to the counter electrode via the load. The whole process is thus regenerative and cyclic.

and 11–12% under diffuse natural daylight [6]. Calculations which consider the spectrum of the light utilized by the dye indicate that low cost cells of at least 10% efficiency could be realized [11,12]. What will be presented in this paper is that cells of at least 6% efficiency can indeed be produced using these techniques. Preliminary analysis presented in this paper estimates that a *stable* 10% efficient module could produce power at $0.6 per peak watt, allowing the nanocrystalline solar cell to be competitive with conventional fossil fuel sources.

2. Experimental methods

The experimental methods for the fabrication of the cell were similar to the procedures found in the literature [9,10]. A pre-scribed 2 cm wide plate ($\cong$ 4 cm long) of 10 Ohm/square conducting glass (Libbey Owens Ford SnO_2:F coated) was used as the substrate for the deposition of the TiO_2. The plate was scribed down the middle and at 1 cm intervals along the length plate. Scotch adhesive tape ($\cong$ 40 μm) was applied to the two longer sides of the glass so that one cm was masked on each edge. A drop (5 μl/cm^2) of titanium butoxide or $TiCl_4$ (10 mM in isopropanol) was distributed on the plate, by sliding a glass rod over the substrate, and allowed to air dry. A droplet (5 μl/cm^2) of a water solution of TiO_2 was then distributed uniformly on the plate. Similarly to commercial paint manufacture, the solution was created by grinding 0.4 ml of acetylacetone into colloidal (P25 Degussa) TiO_2 powder with a mortar and pestle and then slowly adding 20 ml of water while grinding. Before applying the TiO_2, 0.2 ml of Triton X-100 surfactant was gently mixed into the solution. The viscosity of the colloidal TiO_2 solution was found to be between 15–20 mPa-s using a Carri–Med Rhevisco CS Rheometer at shear rates of over 1000 s^{-1}. As a reference, the viscosity of water is found to be 1 mPa-s. The TiO_2 coated glass plate was fired in an air stream at 450°C for 30 min in order to sinter the film. Similar to the procedure in the literature [9,10] the film was then cooled and treated with a 50 ml/cm^2 solution of 0.2 M $TiCl_4$ for 1 h, washed with water, and annealed again at 450°C for 30 min. The titanium butoxide solution used in the pre-coating step was also found to substitute well for the $TiCl_4$ if it was allowed to react on the colloidal film for only 1 min. The completed TiO_2 coated substrate was then broken into 1×1 cm pieces, and plunged while still warm into a 5×10^{-5} M ethanol solution of the ruthenium trinuclear dye [13]. The colloidal TiO_2 film, shown in Fig. 4a, was found to have a thickness of 7–10 μm, and was found to consist primarily of the anatase phase with 20% rutile. The ethanol used was reagent grade and was kept dry by using a few beads of a molecular sieve. After 8 h, the coated plate was removed, washed with ethanol, and dried in a stream of nitrogen. A drop of the electrolyte solution, was quickly placed on the TiO_2, and the counter electrode was placed on top as shown in Fig. 1. The length of the cell was 1 cm, and the final active area of the device was 1×0.5 cm^2. The electrolyte consisted of 0.5 M tetrapropylammonium iodide and 0.05 M iodine in ethylene carbonate and water free acetonitrile. The solid ethylene carbonate was 70–80% by volume and was dissolved in the acetonitrile before the other compounds were included. Propylene carbonate, substituted for the acetoni-

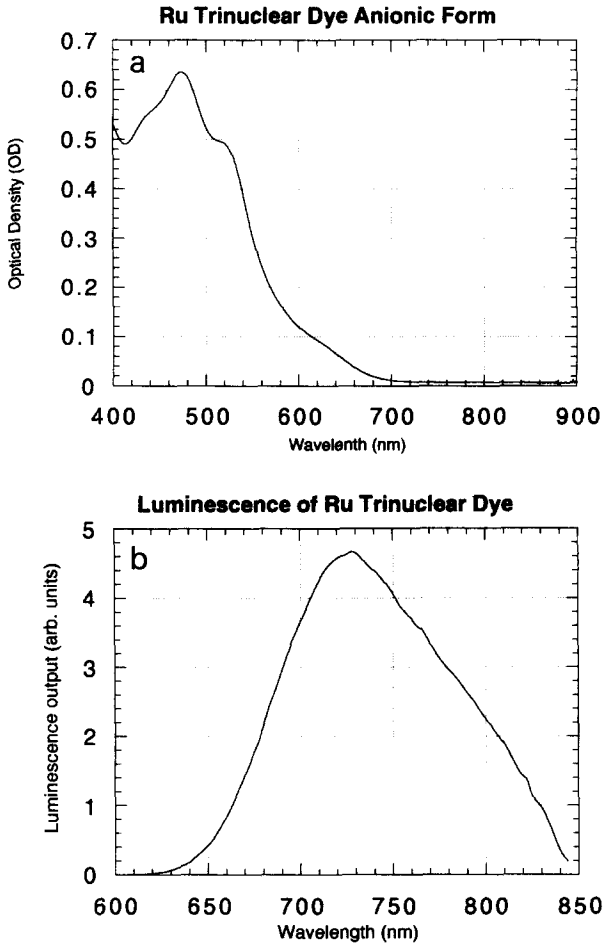

Fig. 4. Ru trinuclear dye: (a) optical absorption spectra for a 10^{-5} M Ru dye solution in ethanol, which possesses a broad absorption form 400–700 nm (newer Ru dyes [10] absorb farther into the infra red), and (b) photoluminescence emission spectra: the excitation wavelength was 500 nm, the photoluminescence efficiency, Φ, is 5×10^{-3}.

trile, yielded similar results, although currents and *I–V* curve fill factors were found to be approximately 20% lower under full AM 1.5 illumination. The platinized SnO_2 glass plate counter electrode was produced via electrodeposition from a hexachloroplatinate solution at 20 mA/cm^2 for 1–2 s. As shown in Fig. 2b, the platinum consisted of fined grained, isolated areas on the larger grains of conductive SnO_2.

To prepare the dye [13–16], $Ru(dcbH_2)_2Cl_2$ (0.2 g, 0.3 mmol) was dissolved in 10 ml of water adjusted to pH 7 by the addition of NaOH. The symbols ($dcbH_2$) and (bpy) represent the 2,2′bipyridil-4,4′dicarboxylic acid and the 2,2′bipyridil ligands, respectively. This solution was slowly added to a 120 ml boiling solution of $Ru(bpy)_2CN_2$ (1.4 g, 3 mmol) [15] in methanol. The mixture was refluxed for 18 h.

After the methanol was rotary evaporated, the solution was filtered with the elimination of the unreacted $Ru(bpy)_2CN_2$. Two 5 ml portions of the filtered solution were loaded on two 80×2.5 columns of Sephadex G15 and eluted with water. The first brown fraction was shown to contain the trinuclear complex with residual traces of $Ru(bpy)_2CN_2$ which was eliminated in the subsequent purification steps. The brown fraction was concentrated to 10 ml and the neutral trinuclear complex was precipitated near pH 3 with HCl. The solid was filtered and dissolved in water at pH 7 by adding NaOH. After the solution was concentrated to about 5 ml, 200 ml of acetone was added while stirring. The precipitated sodium salt of the trinuclear complex was filtered and dried in air. The purity of the dye was established using optical absorption and fluorescent emission. UV-Vis spectra were recorded with a Kontron 860 spectrophotometer. Emission spectra were taken with a Perkin-Elmer MPF 44E spectrofluorimeter equipped with a Hamamatsu R 928 tube. The emission spectra were corrected for the instrumental response by calibration with a NBS standard quartz-halogen lamp. Current–voltage (I–V) curves were measured using a variable load while the cell was illuminated at AM 1.5 1000 W/m^2 by an Oriel solar simulator. Additional indoor measurements were carried out using a more primitive light source consisting of a 250 W tungsten halogen lamp equipped with a UV blocking Schott 395 filter and an IR absorbing water solution of 0.1 M $CuSO_4$ contained in a cuvette of 1 cm pathlength. These measurements were compared with those taken using natural sunlight on the roof of the Paul Scherrer Institute in August. Irradiance values were measured using a Kipp and Zonen CM11 pyranometer. The automated outdoor testing facility set up has been described elsewhere [17].

3. Results and discussion

3.1. Experimental results

Fig. 4a shows the absorption spectrum of a 3.6×10^{-5} M ethanolic solution of the trinuclear complex $Na_2[(NC)Ru(bpy)_2\ (CN)Ru(dcb)_2(NC)Ru(bpy)_2CN)]$. The complex displays a solvatochromic behavior due to the presence of the two terminal cyanide ligands. The most intense absorption band, at 480 nm, is attributed to metal to ligand charge transfer transitions, MLCT, localized on the external NC–$Ru(bpy)_2$–CN units, and is blue shifted to 420 nm in water [13]. The intense shoulder at 520 nm is assigned to MLCT transitions on the Ru(dcb) unit [13], while the weaker absorption is probably due to spin forbidden transitions to ^{3}MLCT states, being that this band is near the energy of the onset of the emission spectra (see Fig. 4b). The luminescent emission shown in Fig. 4b is attributed to the radiative relaxation of an excited ^{3}MLCT localized on the central unit as was demonstrated by time resolved Raman measurements to be reported in a subsequent paper [18]. The emission yield or photoluminescence efficiency, Φ, observed in ethanol is 5×10^{-3} relative to $[Ru(bpy)_3]^{3+}$ which has a Φ value of approximately 0.06 [19]. No luminescence was observed from the finished cell, or from the ethanol washed dye and TiO_2 electrode assembly. Luminescence was observed

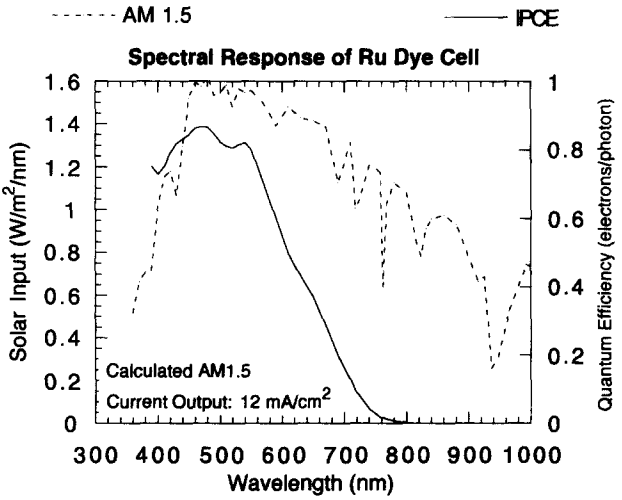

Fig. 5. Air Mass 1.5 Solar Spectrum and measured photocurrent efficiency (IPCE) for the Ru Trinuclear dye as a function of wavelength. This was used to obtain the predicted photocurrent of 12 mA/cm^2 for the Ru trinuclear dye–TiO_2 solar cell.

from the electrode assembly if more concentrated solutions were used for the dye attachment process or if the electrode was not well washed with ethanol. We, therefore, attribute residual luminescence to non-injecting or free dye molecules. This will be further discussed in Section 3.2.2.

Fig. 5 shows a current collection, or Induced Photo-current Collection Efficiency, or IPCE, for a typical cell incorporating the Ru trinuclear dye. This is

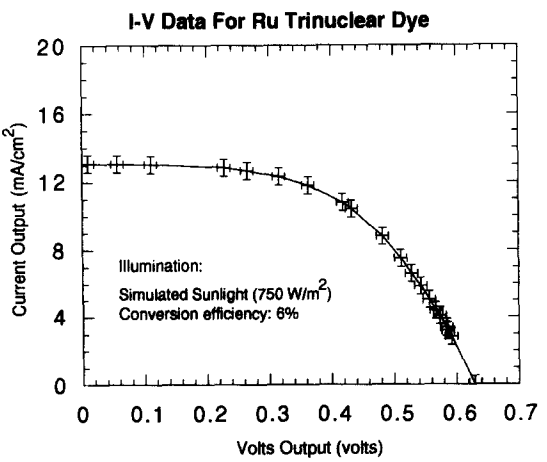

Fig. 6. Typical experimental current voltage curve for the Ru dye cell under illumination by a filtered tungsten halogen lamp (750 W/m^2). While the efficiency under daylight is lower than 6%, this plot demonstrates that high photocurrents and voltages are possible with TiO_2–Dye cells in agreement with the literature [6].

Table 1
Summary of highest values for $I-V$ curve measurements using the Ru trinuclear dye on high surface area TiO_2

Conditions	I_{sc} (mA/cm^2)	V_{oc} (V)	FF	Efficiency
Best Indoor 750 W/m^2 Tungsten Halogen	13.1	0.63	0.55	5 –6%
Best Solar Simulator AM 1.5 1000 W/m^2	10.2	0.68	0.63	4.4–5%
Best Outdoor 470 W/m^2	6.3	0.61	0.61	5 –6%
Best Outdoor 900 W/m^2	11.2	0.68	0.49	4.2–5%

expressed as the ratio of electrons produced to incident photons. These measurements utilized a calibrated Silicon detector to measure the number of photons present at each wavelength [20]. Fig. 6 shows one of the best measured $I-V$ curves for the finished dye cell taken using the tungsten halogen lamp arrangement. As measured by the C11 pyranometer, the illumination at the cell was 750 W/m^2 as was used previously [6]. The cells in the present study had a mirror placed in back of the counter electrode to enhance the absorption of long wavelength photons as is done with the back contact of high efficiency Silicon cells [20]. The resulting fill factor, FF, was 0.55, the open-circuit voltage, V_{oc}, was 0.63 V and the short-circuit current, I_{sc}, was 13.1 mA/cm^2. This resulted in a solar conversion efficiency of 5–6%. The error bars in Fig. 6 and the range given for the efficiency is due to the variation of cell output over 30 min. If the illumination levels were increased to 1000 W/m^2 as is standard in photovoltaics [20,21], the FF decreased, resulting in an efficiency of between 4–5%. The possible cause of this dependence of efficiency and fill factor on illumination will be discussed in Section 3.2.1. Table 1 shows a summary of the best measurements done under various illumination conditions. It was often observed that the currents and voltages measured within the first few seconds were higher than the "stabilized" efficiencies taken 5–10 min. after the cell was assembled. The range given for efficiencies thus represents variation over time and also considers the optical losses of the plastic cover used in the dye cell holder (i.e., an 90% transmission). As can be seen from this table, the voltage and photocurrent values are in the range previously reported for this Ru dye [6].

3.2.1. Discussion of I–V curve results

It is well known that the efficiency of any photoconverter is a function of the incident spectral distribution and light intensity [20,21]. This may explain some of the differences between the efficiency values previously reported and those measured in the present study. In the end, the most significant and useful measurements are those taken using actual daylight. In order to validate the photocurrent measurements, a simple calculation was performed in order to estimate the expected photocurrent from the spectral response of the dye. The optical absorption of the dye shown in Fig. 4a will be influenced by the nature of the species in

Table 2
Summary of the experimental I_{sc} and solar conversion efficiency values in comparison to predictions made using the AM 1.5, 1000 W/m^2 spectrum, and assuming FF = 0.7, and V_{oc} = 0.7 V. The predicted current is calculated from the AM 1.5 spectrum assuming one electron created per absorbed photon. The normalized IPCE is the spectrum obtain from the IPCE data shown in Fig. 5 divided by the maximum IPCE value

Conditions	Current (mA/cm^2)	Efficiency
Literature [6] ("AM 1.5" 750 W/m^2)	11.5	7%
Present Study (AM 1.5 1000 W/m^2)	9 –12	3–5%
Predicted from IPCE data	12	5–6%
Predicted from IPCE (normalized)	14	6–7%
Predicted from IPCE = 1 (400–650 nm)	15 –16	7–8%
Predicted from IPCE = 1 (400–750 nm)	22	10–11%
Predicted from IPCE = 1 (400–800 nm)	25 –26	12–13%
Predicted from IPCE = 1 (360–1100 nm)	42 –43	20–21%

the vicinity of the dye as well as the concentration of the dye. The absorption of the final cell will be influenced by these factors, as well as the geometry of the device, which in turn determines the extent of light trapping and multiple reflections [12,20]. Therefore, the most relevant spectral response data is not found from Fig. 4a, but instead can be found from the ratio of the electrons out per input photon, IPCE, of the actual finished cell. One can convert the known AM 1.5 (1000 W/m^2) solar input power, shown in Fig. 5, into a photon flux by dividing by the photon energy at each wavelength. The maximum photocurrent output, I_{sc}, is then found from the integral over wavelength of the product of the IPCE and the converted Air Mass 1.5 solar spectrum [20]. If *all* AM 1.5 photons in the range from 400–650 nm (750 nm) could be collected (IPCE = 1) a current of 16 mA/cm^2 (22 mA/cm^2) would be expected. If one uses the actual photo current (IPCE) spectra shown in Fig. 5, 12 mA/cm^2 is obtained in agreement with the measured values. These calculations are summarized in Table 2 and suggest that with respect to photocurrent, the cell behaves as expected. The calculations also suggest that newer dyes [10] which utilize more of the solar spectrum can yield cells of over 10% efficiency.

Another difference to be explained is the lower fill factors observed (0.6 in Table 1 versus 0.7 in Ref. [6]) which may be due to the porosity of the TiO_2 layers used and the kinetics of the diffusion of the electrolyte through the membrane. In the present study, commercial nanometer sized particles of TiO_2 (see [9,10]) were used, in contrast to the sol gel material used in the initial work [6]. As mentioned in Section 3.1., the fill factor, FF, and conversion efficiency decreased with increasing light intensity and when a solvent of higher viscosity was used instead of acetonitrile. This has also been previously reported for nanocrystalline solar cells [6,9,10]. Clearly, the redox couple in the electrolyte must transfer electrons at the rate that they are being injected. A possible reason for decreased performance is thus the series resistance of the cell which is in part due to the slow diffusion of the triiodide–iodide redox couple, and in part due to the sheet resistance of the conductive glass. A load resistor in "internal series" with the cell

is known to effect the cell near the higher voltage values in the I–V plot [12,20]. From this region of Fig. 6, a resistance value of approximately 40 Ω is obtained. As the light intensity is decreased, the current through this resistor is decreased and it's effect on the I–V curve is less noticeable. The value of the resistance due to diffusion may itself decrease at lower current densities found under lower illumination. Another factor to consider is the spectrum of the incident light. As can be seen in Fig. 5, the cell is sensitive from 400 to 750 nm. The AM 1.5 spectrum shown in this figure is not the spectrum one obtains on a cloudy day [20]. If sunlight passes through clouds, the spectrum is modified by the molecular absorption of water, which absorbs weakly in the visible, and strongly in the IR (800–3000 nm). The absorption of water will increase the fraction of the total radiation within 400–750 nm. Since the conversion efficiency is the ratio of the power produced to the total incident solar power, this will result in an increase in the measured efficiencies. One sees from this that it is very important to specify the measurement conditions for the nanocrystalline, and all, solar cells [21].

3.2.2. Discussion of photoluminescence

As previously mentioned, for the experiential conditions used, no detectable photoluminescent emission was detected from the finished cell at open- or closed-circuit, indicating that the excited state of the Ru dye is effectively quenched by the TiO_2. This is in contrast to solid state or photoelectrochemical solar cells such as CdS, a:Si, Si, and GaAs which show at least weak luminescence [11,12]. One can estimate the expected photoluminescence efficiency from the lifetime, τ, of the excited state of the Ru dye molecules adsorbed on TiO_2, which is given in Ref. [22]

$$1/\tau = k_{inj} + k_r + k_{nr}, \tag{1}$$

where k_{inj}, k_r, and k_{nr} are the rate constants for electron injection, radiative and non radiative recombination to the ground state of the excited Ru complex, respectively. The photoluminescence efficiency of the injecting dye molecules in the solar cell is given by

$$\Phi_{cell} = \eta k_r \tau, \tag{2}$$

where η is the inter-system crossing efficiency (from singlet to triplet states), which is thought to be unity for the Ru bpy dyes [13,18]. Similarly, the photoluminescence efficiency of the free dye is given by

$$\Phi_{free} = \eta k_r \tau_0 = \eta k_r/(k_r + k_{nr}). \tag{3}$$

The measured lifetime of the free dye, τ_0, in ethanol is [13,16] 320 ns, and the measured photoluminescence efficiency is 5×10^{-3}. One thus obtains $k_r = 1.6 \times 10^4$ s^{-1} and $k_{nr} = 3.3 \times 10^6$ s^{-1} from Eq. (3). If τ is in the range of 10–100 ps, which leads to $k_{inj} = 10^{11}$ to 10^{12} s^{-1} [6,23], one would estimate that the Φ value for the finished cell is in the range of 10^{-8} to 10^{-7}, which is beyond the instrument detection limits of 10^{-5} to 10^{-6}. Such a large rate constant for charge injection has indeed been inferred from the nearly identical values for the fraction of the light absorbed at each wavelength, i.e., the absorptivity [11,12], and IPCE for the finished cell [6,9,10]. From Eqs. (1–3) one sees that Φ_{cell} is approximated by the ratio of the radiative to injection rate constants. The lack of observed photolumi-

Table 3
Nanocrystalline solar cell module cost estimate breakdown. The cost is calculated per unit module area

Item	Need per m^2	\$ per m^2
TiO_2	10 g Anatase	0.03
Ru Dye [6,13,16]	100 mg adsorbed	7–10
SnO_2:F Glass	2 m^2 (10 Ω/square)	30
Pt for counter electrode	3 monolayers	0.01
Electrolyte and iodide	50 ml	0.1–1
Additional costs:		
Production Overhead (Equipment Depreciation, Indirect and Other Direct Materials)		5–7
Labor (Direct and Indirect which includes assembly and testing)		0.3–0.5
Encapsulant or Sealant		2–3
Frame and electrical interconnects		2
Additional protective glass cover and Tedlar backing		2–3
Profit, Interest due on loans		0–8
Total module cost		48–64 \$/m^2
Cost per peak Watt		0.48–0.80 \$/Wp

nescence from the cell thus points to a charge injection process which is much faster than radiative and non radiative recombination in the free dye. The possible implications of the quenching of the excited state on the predicted photovoltages will be discussed in a subsequent paper.

3.3. Estimated dye cell cost

As a rough estimate of the cost of this new cell, one considers the materials and fabrication costs associated with it's production. This is outlined in Table 3, and uses costs for amorphous silicon solar cells as a guide [24,25]. The cost of the cell is estimated to lie in the range from \$48 to \$64 1993 dollars per square meter. The direct costs such as tools and labor are related to the actual production of the module, while the indirect costs such as accountants, rent, and computers are volume insensitive. This calculation assumes a 5–10 MW_p/year factory with 100 employees, and a capital cost of equipment of \$17,000,000, housed in a 2,000 m^2 facility [24,25]. The module costs are determined primarily by the cost of the conductive glass, and the production overhead. To estimate the cost per peak watt, one relates the cost per unit area with the power produced, which depends on the solar conversion efficiency and the peak solar illumination [20]. For the module alone, an 8% efficient cell would produce power at 0.60–0.80 \$/W_p if the module cost is 48–64 \$/m^2. For a 10% efficient cell, the cost would be approximately 0.48–0.64 \$/W_p. As a comparison, the module costs for single crystal Silicon cells are now 3–8 \$/W_p. To produce useful power in a commercial application, one must consider the average illumination, instead of the peak, as well as the additional costs of land, batteries, support structures *and* the lifetime of the panel.

If these Balance of Systems (BOS) costs [24,25] are considered, the cost of power produced with this solar cell would be 0.07–0.10 $/kWh, assuming a 10% efficient module which lasts at least 15 y under the illumination found in the western United States. These costs do not consider that the nanocrystalline dye solar cell may be more easily recycled than conventional solar cells. Note that this cost lies in the range of electricity costs for conventional fossil fuel based systems, and thus the above analysis demonstrates that the nanocrystalline dye solar cell, if proven to be stable over 15 y, could represent a viable energy option.

4. Conclusions

In this paper it has been demonstrated that using the procedure in the literature, solar cells of at least 6% can be fabricated using an amazingly simple procedure. The confirmation of the efficiencies for this cell is also being demonstrated in other labs [26,27]. Experiments using a derivative of Chlorophyll [9] adsorbed on TiO_2 have produced green colored solar cells with voltages of over 0.5 V and currents of over 9 mA/cm^2. These solar cells can be fabricated in many school science classrooms and can serve as a model system to study electron transfer, photosynthesis and solar conversion. The high photocurrents may not be limited to the Ru dye used in this study or even to organic molecules [28]. Future research should, therefore, focus on the new sensitizers, and the commercialization, reliability and longevity of the cell. Laboratory cells in which the two glass plates have been sealed by a material such as silicone or epoxy have demonstrated that the cell can operate for several months without degradation, however, the sealing of the cell, which contains a liquid electrolyte, remains to be demonstrated under rigorous long term outdoor testing. One approach could involve the evaluation of sealants which can provide a barrier for the evaporation of the electrolyte as well as to the outside environment. Another research approach could involve the replacement of the liquid electrolyte with a transparent solid which will serve as a conductor of positive charge. One class of solid materials which can be investigated are electrically or ionically conducting polymers, such as those developed for electrochromic windows. Given that the current world energy use is expected to increase from 13 terawatts in 1990 to over 19 terawatts in 2026 [29], nanocrystalline dye solar cells could be a sensitive way to capture more that just photographs.

5. Acknowledgement

The economic analysis was provided by Cowan and Associates of San Francisco. The authors would like to acknowledge the assistance of Dr. Michael Graetzel, Andreas Kay, and Paul Liska of the EPFL. The *I–V* curve measurements were performed with the assistance of Dr. W. Durish, Dr. W. Rehwald, and J. Ulm at the PSI. Thanks go to V. Shklover of the ETH Zurich for the SEM analysis and to M. De Giorgi for the viscosity measurements.

6. References

[1] H.W. Vogel, Ber. Dtsch. Chem. Ges. 6 (1873) 1320; B. Elvers, S. Hawkins and G. Schulz, Ullmann's Encyclopedia of Industrial Chemistry A20 (VCH publishers, Cambridge, 1990).
[2] E. Becquerel, Comptes Resdues 9 (1839) 561.
[3] J. Loferski, Progress in Photovoltaics: Research and Applications, 1 (1993) 67–78.
[4] K. Zweibel, Harnessing Solar Power: The Photovoltaics Challenge (Plenum Press, New York 1990).
[5] H. Tributsch and M. Calvin, Photochem. Photobio. 14 (1971) 95 (and references therein).
[6] B. O'Regan and M. Graetzel, Nature 353 (1991) 737–739; M. Graetzel, Comments Inorg. Chem. 12 (1991) 93–111; A. Mueller et al. (Eds.), Studies in Physical and Theoretical Chemisty, Vol. 78, Electron and Proton Transfer in Chemisty and Biology (Elsevier, Amsterdam, 1992).
[7] M. Graetzel and P. Liska, Photo-electrochemical cell and process of making same, US Patent No. 5,084,365, 1992; Scientific American, January 1992, p. 138; M. Graetzel, The World and I, The Washington Times Corp. (February 1993) 228–235.
[8] D. Bradley, Science 259 (1993) 890–892.
[9] A. Kay and M. Graetzel, J. Phys. Chem. 97 (1993) 6272–6277.
[10] M.K. Nazeeruddin, A. Kay, I. Rodicio, R. Humphry Backer, E. Mueller, P. Liska, N. Vlachopoulos and M. Graetzel, J. Am. Chem. Soc. 115 (1993) 6382–6390.
[11] G. Smestad, in: Proc. SPIE Conf. on Energy Efficiency and Solar Energy Conversion XI, Toulouse, France, 18–22 May, 1992, (SPIE, Bellingham, Washington, 1992); Proc. SPIE Conf. on Energy Efficiency and Solar Energy Conversion XII, San Diego, USA, 13–14 July, 1993 (SPIE, Bellingham, Washington, 1993).
[12] G. Smestad and H. Ries, Sol. Energy Mater. Sol. Cells 25 (1992) 51–71.
[13] R. Amadelli, R. Argazzi, C. Bignozzi and F. Scandola, J. Am. Chem. Soc. 112 (1990) 7099.
[14] P. Liska, N. Vlachopoulos, K. Nazeeruddin, P. Comte and M. Graetzel, J. Am. Chem. Soc. 110 (1988) 3686.
[15] J.N. Demas, T.F. Turner and G.A. Crosby, Inorg. Chem. 8 (1969) 674.
[16] M. Nazeeruddin, P. Liska, J. Moser, N. Vlachopoulos and M. Graetzel, Heletica Chemica Acta 73 (1990) 1788.
[17] W. Durisch, Verband Schweizerischer Electrizitatswerke, SEV/VSE 10/1993.
[18] C.A. Bignozzi, R. Argazzi, C. Chiorboli, F. Scandola, R.B. Dyer, J.R. Scoonover and T.J. Meyer, Inorg. Chem., in press.
[19] A. Juris, V. Balzani, F. Barigelletti, S. Campagna, P. Belser and A. Von Zelewsky, Coord. Chem. Rev. 84 (1988) 85–277.
[20] C. Hu and R.M. White, Solar Cells From Basics to Advanced Systems (McGraw Hill, San Francisco, 1983) p. 106–107.
[21] M. Green and K. Emery, Progress in Photovoltaics: Research and Applications 1 (1993) 25–29.
[22] K. Hashimoto, M. Hiramoto. A. Lever and T. Sakata, J. Phys. Chem. 92 (1988) 1016–1018.
[23] F. Willig, R. Eichberger, N.S. Sundaresan and B.A. Parkinson, J. Am. Chem. Soc. 112 (1990) 2702; R. Eichberger and F. Willig, Chem. Phys. 141 (1990) 159; F. Willig, R. Kietzmann and K. Schwartzburg, in: Proc. SPIE Conf. on Energy Efficiency and Solar Energy Conversion XI, Toulouse, France, 18–22 May, 1992, (SPIE, Bellingham, Washington, 1992).
[24] D. Coiante and L. Barra, Sol. Energy Mater. Sol. Cells 27 (1992) 79–89.
[25] J. Ogden and H. Williams, Int. J. Hydr. Energy 15 (1990) 115–169.
[26] A. Hagfeldt, Microporous and polycrystalline semiconductor electrodes studied by photo electrochemical methods supported by quantum chemical calculations and photoelectron spectroscopy, PhD Thesis, Uppsala University Sweden, ISBN 91 554 30430, 1993; A. Hagfeldt et al., Sol. Energy Mater. Sol. Cells 31 (1994) 481–488.
[27] R. Knodler, J. Sopka, F. Harbac and H. Grunling, Sol. Energy Mater. Sol. Cells 30 (1993) 277.
[28] S. Hotchandani and P. Kamat J. Phys. Chem. 96 (1992) 6834–6839.
[29] L. Schipper and S. Meyers, Energy Efficiency and Human Activity (Cambridge University Press, Cambridge, 1992) p. 1–47.